DR. KATHARINE MARSKE (Orcid ID : 0000-0002-9837-9367)

Article type : Original Article

Dispersal barriers and opportunities drive multiple levels of phylogeographic concordance in the Southern Alps of New Zealand

Katharine A. Marske[1,2]*, Andréa T. Thomaz[2,3,4], L. Lacey Knowles[2]

[1] *Department of Biology, University of Oklahoma, Norman, OK, 73019, USA*

[2] *Department of Ecology and Evolutionary Biology, University of Michigan, Ann Arbor MI, 48109, USA*

[3] *Biodiversity Research Centre and Department of Zoology, University of British Columbia, Vancouver, BC, V6T 1Z4, Canada*

[4] *Current address: Facultad de Ciencias Naturales, Universidad del Rosario, Bogotá DC, Colombia, 111221*

**Corresponding author: kamarske@ou.edu*

Abstract

Phylogeographic concordance, or the sharing of phylogeographic patterns among co-distributed species, suggests similar responses to topography or climatic history. While the orientation and timing of breaks between lineages are routinely compared, spatial dynamics within regions occupied by individual lineages provide a second opportunity for comparing responses to past events. In environments with complex topography and glacial history, such as New Zealand's South Island, geographically nested comparisons can identify the processes leading to phylogeographic concordance between and within regional genomic clusters. Here, we used single nucleotide polymorphisms (obtained via ddRADseq) for two co-distributed forest beetle species, *Agyrtodes labralis* (Leiodidae) and *Brachynopus scutellaris* (Staphylinidae), to evaluate the role of climate change and topography in shaping phylogeographic concordance at two, nested spatial scales: do species diverge over the same geographic barriers, with similar divergence times? And within regions delimited by these breaks, do species share similar spatial dynamics of directional expansion or isolation-by-distance? We found greater congruence of phylogeographic breaks between regions divided by the strongest dispersal barriers (i.e., the Southern Alps). However, these shared breaks were not indicative of shared spatial dynamics within the regions they delimit, and the most similar spatial dynamics between species occurred within regions with the strongest gradients in historical climatic stability. Our results indicate that lack of concordance as traditionally detected by lineage turnover does not rule out the possibility of shared histories, and variation in the presence and type of concordance may provide insights into the different processes shaping phylogeographic patterns across geologically dynamic regions.

Introduction

A primary interest in the study of comparative phylogeography is the extent to which co-distributed species have responded similarly to past events and to characteristics of the landscape (Avise et al., 1987; Bermingham & Moritz, 1998; Papadopoulou & Knowles, 2016; Rissler, 2016). Complex landscapes have been shown to generate complex spatial and demographic histories (Binks, Gibson, Ottewell, Macdonald, & Byrne, 2019; Carnaval et al., 2014; Massatti & Knowles, 2016; Paz et al., 2018), driving varying levels of phylogeographic concordance between co-distributed species. In such landscapes, similarity between species may be apparent at different spatial scales, from phylogeographic breaks and divergence times shared between lineages (Ellis et al., 2015; Moritz et al., 2009; Oswald, Overcast, Mauck, Andersen, & Smith, 2017; Rissler & Smith, 2010) to spatial or temporal dynamics of individual geographic lineages (Prates et al., 2016; Thomaz & Knowles, 2020). While patterns of turnover between lineages have been described for many systems, the spatial dynamics within the regions delimited by these breaks are typically less scrutinized. However, these regional dynamics

are no less critical in understanding species responses to environmental change and the role of landscape features in driving diversification because they clarify the processes by which individual regions accumulate diversity (Carnaval et al., 2014) and provide the historical backdrop for regional community assembly (Bermingham & Moritz, 1998; Marske, Rahbek, & Nogués-Bravo, 2013).

Beyond the impacts of features expected to drive lineage turnover —dispersal barriers or multiple refugia— it is difficult to generalize predictions for spatial or demographic phylogeographic concordance among co-distributed species which are ecologically similar but do not appear to share tight biotic interactions (Burbrink et al., 2016; Carstens & Richards, 2007). Even suites of co-evolved species (e.g., pollination syndromes and other mutualisms; parasites or parasitoids and their hosts) show a range of comparative phylogeographic patterns, from "evolutionary communities" which move through time and space together (Satler & Carstens, 2019; Smith et al., 2011), to intermediate histories where only some members of a pollination syndrome share spatial and demographic histories (Espíndola, Carstens, & Alvarez, 2014), to distinctly different spatial patterns or ecological constraints among hosts and parasites/parasitoids during postglacial expansion (Bunnefeld, Hearn, Stone, & Lohse, 2018; Tsai & Manos, 2010). For non-co-evolved species, where expectations for concordance are shaped solely by shared responses to the environment, the generality of phylogeographic patterns is likely extremely contingent upon the landscape in which they occur (Rissler, 2016) or ecological similarities among species (Papadopoulou & Knowles, 2016).

So, should concordance be the null expectation for co-distributed species? It depends. Species subject to similar environmental conditions in the same space may (Moritz et al., 2009; Salces-Castellano et al., 2019) or may not (Ellis et al., 2015; Marske, Leschen, & Buckley, 2012) share lineage boundaries, depending on the structure of the landscape. For example, where mountains and other features reflect hard barriers to dispersal, species are more likely to share phylogeographic breaks (Pyron & Burbrink, 2010), but different lineages are affected by these common barriers in different ways and at different rates (Smith et al., 2014; Thomaz & Knowles, 2020). Finally, phylogeographic concordance at one level (e.g., phylogeographic breaks) does not indicate concordance at others (e.g., spatial or demographic patterns within the regions delimited by those breaks) (Garrick, Rowell, Simmons, Hillis, & Sunnucks, 2008), and glacial refugia that are shared among species may preserve the signal of previous idiosyncratic divergence histories, rather than recent climatic cycles (Wallis & Trewick, 2009). Comparative phylogeographic patterns between and within lineages therefore yield different

information on how organisms respond to dynamic environments, and concordance likely varies across species' distributions under different sets of conditions.

Due to its dynamic geological history of Pliocene mountain building followed by Quaternary glaciation (reviewed by Wallis, Waters, Upton, & Craw, 2016), New Zealand' South Island is a model system for investigating the impacts of dispersal barriers and variation in environmental stability on phylogeographic concordance at different scales. At the regional level, South Island is divided longitudinally by the Southern Alps forming a dispersal labyrinth of high mountains intercalated by small remnants of Pleistocene glaciers, narrow alpine zones separating mountain beech forests (e.g., Arthurs Pass), and low mountain passes that connect eastern and western forests (e.g., Haast Pass) (Figure 1). These features have served as important drivers of diversification (Craw, Upton, Burridge, Wallis, & Waters, 2016; Dennis, Dunning, Sinclair, & Buckley, 2015; Fernández & Giribet, 2014). Likewise, a diversity of phylogeographic patterns and high degree of mitochondrial genetic structure among South Island arthropods indicates that many persisted through the Last Glacial Period in multiple refugia (Boyer, Baker, & Giribet, 2007; Marshall, Hill, Fontaine, Buckley, & Simon, 2009; Marshall et al., 2012; McCulloch, Wallis, & Waters, 2010; O'Neill, Buckley, Jewell, & Ritchie, 2009; Pons et al., 2011). For many species, these refugia preserved existing phylogeographic structure, with lineage divergence predating the Last Glacial Maximum (Buckley, Krosch, & Leschen, 2015; Wallis & Trewick, 2009). Thus, the geographic contrasts afforded by South Island's dynamic landscapes—regions with glacial refugia and hard barriers to dispersal (northern South Island), juxtaposed against regions with no known forest refugia, for which surrounding barriers are more permeable and therefore species-specific in impact (southern South Island)—have driven a diversity of phylogeographic patterns, allowing a systematic test of the features likely to result in phylogeographic concordance between and within geographic regions.

We investigate the depth of concordance between two New Zealand forest beetles with similar life histories, but no direct interaction: *Agyrtodes labralis* (Broun, 1921) (Leiodidae) and *Brachynopus scutellaris* (Redtenbacher, 1868) (Staphylinidae: Scaphidiinae). Both species complete their life cycles on saproxylic fungi and are widely co-distributed across South Island, although *B. scutellaris* are apparently absent from the Westland *Nothofagus* gap, an area of the west coast from which Southern Beech forests are absent (Leschen, Buckley, Harman, & Shulmeister, 2008). A previous study (Marske et al., 2012) based on mitochondrial DNA demonstrated the importance of the Southern Alps and intervening mountain passes in structuring lineages for each species, with a lack of concordance in the orientations of lineages and breaks—despite persistence in many of the same glacial refugia (Figure 1)—indicating different responses to dispersal opportunities. Marske

et al. (2012) also identified species-specific geographic origins for each species followed by a general pattern of recent dispersal into Southland, suggesting that concordance varies geographically based on differences in the processes shaping genetic diversity among regions (e.g., environmental stability and population persistence; environmental change and range expansion or shift).

Here, we explicitly test the factors that promote phylogeographic concordance across species' distributions. Specifically, we use single nucleotide polymorphisms (SNPs) to ask whether *A. labralis* and *B. scutellaris* show similar phylogeographic patterns at two, nested spatial scales: *Across South Island*, do shared phylogeographic breaks correspond to hard geographic barriers, such as large mountain ranges? Do they share divergence times? *Within regions* delimited by these breaks, do species share similar spatial dynamics (e.g., directional expansion or isolation-by-distance)? Is concordance conditioned upon climate history? These questions allow us to juxtapose roles of dispersal limitation and opportunity in shaping spatial patterns of genomic divergence and identify the extent to which phylogeographic concordance indicates the influence of similar processes in shaping that structure. We predict that detection of concordance in lineage turnover will vary based on the strength of barriers to dispersal and will be strongest in central South Island along the Southern Alps, while concordance in regional spatial dynamics will be more closely associated with similar histories of recent dispersal than long-term environmental stability and will be strongest in the south. As such, our study implicates processes acting at different temporal scales and spatial extents in driving phylogeographic concordance at multiple levels.

Methods

Genomic Library Preparation

Genomic DNA for *A. labralis* and *B. scutellaris* were selected among samples available from previous studies (Leschen et al., 2008; Marske, Leschen, Barker, & Buckley, 2009; Marske et al., 2012). All samples were retrieved from the New Zealand Arthropod Collection (Landcare Research, Auckland, New Zealand) after a minimum of 6 years stored in DNA elution buffer at -80°C. From the 189 and 340 samples available, respectively, 100 individuals with ~100 ng DNA template available, following the recommendations of Peterson, Weber, Kay, Fisher, & Hoekstra, 2012, were selected from across each species' South Island distribution (although a few samples fell below 100 ng DNA; see Supplementary Methods). Samples were selected to ensure the inclusion of representatives from multiple mitochondrial lineages, particularly where lineages overlapped. For *B. scutellaris*, we also included four individuals from North Island to assess

independence of the evolutionary histories of South and North Islands for this more broadly distributed species (see Supplementary Methods for details about sample selection).

Briefly, DNA was digested with the restriction enzymes EcoRI and MseI. Unique barcodes were ligated to the digestion fragments, which were then pooled. DNA fragments between 350-450 bp were selected from the pooled samples using Pippin Prep (Sage Science, Beverly, MA), and the size-selected samples were then amplified via 8-10 PCR cycles to incorporate Illumina adapter sequences. All steps were followed by cleaning using AMPure beads (1.6x ratio; except after Pippin Prep) and a high sensitivity Qubit quantification assay. Each library (one per species with 100 individuals each) was sequenced in one lane of an Illumina HiSeq2500 to generate single-end 150-bp reads at the Centre for Applied Genomics (Hospital for Sick Children, Toronto, Canada).

Processing of Illumina Data

Sequences were de-mutiplexed and single nucleotide polymorphisms (SNPs) were identified for each species separately using the STACKS 1.4.1 pipeline, which calls loci from short-read sequences using a maximum likelihood framework (Catchen, Hohenlohe, Bassham, Amores, & Cresko, 2013). During the de-multiplexing stage (process_radtags), only reads with a Phred score ≥33, one or fewer mismatch in the adaptor sequence, a barcode distance of two, and individuals with >200,000 reads were retained (Thomaz, Malabarba, & Knowles, 2017). Putative loci were determined from the resulting reads for individual beetles (100 *A. labralis*, 98 *B. scutellaris*) in USTACKS using a minimum coverage depth of 5. A catalog of consensus loci was generated using CSTACKS, with up to two mismatches allowed between individuals. SSTACKS then matched individuals against this catalog to identify the alleles present at homologous loci. SNP data for loci present in at least two localities were exported via POPULATIONS (each locality was considered a population). We then used a custom R script (https://github.com/ichthya/ThomazKnowles2020_scripts) to remove SNPs from the final 10 positions of each locus and to identify SNPs at segregating sites with a sharp increase in substitutions and exceptionally variable loci (Θ within the 95th percentile), both of which indicate a probable increase in incorrect calls. We removed these by creating a whitelist input in a second run of POPULATIONS. All STACKS steps were run with eight parallel threads in the University of Michigan Flux.

Because the analyses described below tolerate different thresholds for missing data, we used PLINK 1.07 (Purcell et al., 2007) to extract different subsets of individuals and loci from the second POPULATIONS output. For all data subsets, we first checked for individuals with a high frequency of missed calls, and two *A.*

labralis with approximately four times the missing data of the next highest individual were removed from all subsequent analyses. We next removed loci with the percentage of missing data above a selected threshold (up to 25% unless specified below) for each species; this analysis was carried separately on the regional groups identified below, and for *B. scutellaris* excluding the North Island individuals, to maximize the number of loci shared across individuals for each analysis.

Geographic regions

To identify geographically constrained genomic clusters, we inferred patterns of genetic structure using STRUCTURE 2.3.4 (Pritchard, Stephens, & Donnelly, 2000) without conditioning to any population assignment. Data for each species were analyzed with values of *K* ranging from 1 until the *K*-value at which we observed a stabilization of mean likelihood values, and the maximum *K*-value estimated was 5 and 6 for *B. scutellaris* and *A. labralis*, respectively. For each combination of parameters (i.e., dataset and *K*-value), ten independent runs were performed with 300,000 Markov Monte Carlo iterations and 100,000 as burn-in. For both species, the *K*-value that best fit the data was selected using ΔK (Evanno, Regnaut, & Goudet, 2005) implemented in STRUCTURE HARVESTER (Earl & vonHoldt, 2012). Putative ancestral proportion assigned to each individual was graphically presented using CLUMPAK (Kopelman, Mayzel, Jakobsson, Rosenberg, & Mayrose, 2015).

For *B. scutellaris*, given the strong genomic structure inferred, we also performed hierarchical STRUCTURE analyses within each major genomic cluster. We used only the individuals in each inferred cluster, for which we re-estimated the 25% missing data for the focal individuals only to take advantage of loci unique to each cluster. We also excluded one extraordinarily divergent individual from a northern population at Mt. Arthur (Flora Saddle) which had a strong impact on the number of minor STRUCTURE clusters identified from the hierarchical STRUCTURE analyses and the downstream analyses which used these clusters (see below). *K*-values evaluated in these hierarchical analyses ranged from 1 to 5.

Procrustes test for geographic and genetic association

We tested the strength of the relationship between geography and population genetic divergence using a Procrustes analysis, a multivariate method in which two data matrices are rotated to minimize the Euclidean sum-of-squares differences between them (Wang, Zöllner, Rosenberg, Weinblatt, & Shadick, 2012). Unlike tests of IBD based on Mantel or ddRDA, Procrustes retains the spatial structure of the data, allowing visualization of how deviations from IBD are distributed across the landscape (e.g., in relation to geographic barriers; see Knowles, Massatti, He, Olson, & Lanier, 2016). During Procrustean superimposition the

significance of the relationship between the two matrices is tested via permutation (Peres-Neto & Jackson, 2001; Wang et al., 2012), and this method has been shown to outperform the Mantel test under a variety of conditions (Peres-Neto & Jackson, 2001). Here, the first two Principal Components axes of genetic variation are rotated to match the geographic orientation of sample localities as closely as possible, and the spatial offset between individuals in PC and geographic space represents the extent of deviation from the expected pattern of genetic variation based on geography alone (Knowles et al., 2016; Papadopoulou & Knowles, 2015; Wang et al., 2010, 2012).

Principal components and Procrustes analyses were performed in R using the *adegenet*, *ade4* and *vegan* packages (Dray & Dufour, 2007; Jombart, 2008; Oksanen et al., 2018). Prior to PCA, missing data (maximum of 25%) were replaced by the mean frequency of the corresponding allele (Jombart, 2008). Procrustes transformation of the data was performed in *vegan*, with the first two PC axes of genetic variation and the latitude and longitude of collection localities for all individuals as direct inputs. Significance of the relationship between geography and genetic divergence was assessed using the PROTEST function, which tested the non-randomness between the two configurations via 10,000 permutations (Oksanen et al., 2018). We also performed separate Procrustes analyses for the different genomic clusters identified via STRUCTURE analyses and the initial Procrustes runs for each species.

Directionality test for population expansion

To compare population dynamics among geographic regions, and based on previous studies which suggested population expansion from multiple refugia, we tested for evidence of range expansion using a directionality index, Ψ, which infers the strength and directionality of genetic clines in the allele frequency spectrum (Peter & Slatkin, 2013, 2015). The directionality index allows the detection of recent geographic expansion and estimation of the location of origin (Bemmels, Knowles, & Dick, 2019; Manuel et al., 2016; Pierce et al., 2014). We used the *X-Origin* pipeline in R (He, Prado, & Knowles, 2017) to identify the origin and direction of population expansion within each genomically-defined region, as delimited by the STRUCTURE and Procrustes analyses. Given that inferences of expansion and origin are sensitive to both a small number of populations (leading to artificially high R^2), and to small population sizes, all localities for *A. labralis* and *B. scutellaris* were grouped into 24 and 22 geographically defined 'populations', respectively, based on topographic breaks or sampling gaps independent of the genetic data itself (omitting, in a few instances, single-individual localities that were geographically remote from the next nearest locality; Supplementary Figure 3). We used South Island as the background for inferring expansion, except for the northern cluster for *B.*

scutellaris, for which lower North Island was included, with geographic distances among populations estimated using the Haversine formula.

Temporal concordance of population divergence

To identify whether shared phylogeographic breaks correspond to common temporal origins and to test for the permeability of these breaks for each species, we estimated divergence times across different mountain barriers for two divergence models—with and without migration—using the composite-likelihood method FASTSIMCOAL2 (Excoffier, Dupanloup, Huerta-Sánchez, Sousa, & Foll, 2013; Excoffier & Foll, 2011) based on the folded joint Site Frequency Spectrum (SFS) with pairwise comparisons. First, we tested for simultaneous divergence of *A. labralis* and *B. scutellaris* across the Southern Alps, with localities in the south counted as part of the western group based on STRUCTURE and Procrustes results (Figures 2c and 3d). Localities from northern South Island were excluded due to the preponderance of missing data for *B. scutellaris.* Second, we estimated the relative timing and order of divergence among geographic regions denoted by the STRUCTURE results for each species (Figures 2d and 3e). We used a custom Python script (He & Knowles, 2016) to estimate the joint Site Frequency Spectrum (SFS) for each species based on 15 individuals (10 for the northern group of *B. scutellaris*) from each region, a single SNP per loci and no missing data.

Divergence times were estimated based on two evolutionary models of divergence: strict divergence and divergence with migration. In the latter, two migration parameters were applied (one in each direction). Note that the focus here is on the relative similarity between species at each phylogeographic break and the order of divergences across different breaks, not the absolute timing. As such, while differences in generation times could affect absolute time estimates, an undetected pattern of temporal concordance would require systematic, and in some cases substantial difference in generation times between these ecologically similar species (see Results). To reduce the parameter space and improve accuracy of estimates based on the SFS (see Excoffier & Foll, 2011), we fixed one population size (N_1) based on the nucleotide diversity from the empirical data (i.e., fixed and variable sites π obtained from rerunning POPULATIONS from STACKS for the relevant clusters). These estimates were based on a mutation rate (μ) of 1.05×10^{-8} and 1.47×10^{-8} for *B. scutellaris* and *A. labralis*, respectively, which we calculated using the regression formula for cellular organisms (Lynch, 2010) and genome sizes reported for *Biocrypta prospiciens* (Staphylinidae) and *Ptomaphagus hirtus* (Leiodidae) (Hanrahan & Johnston, 2011). The remaining parameters (N_2, N_{ANC} and T_{DIV}, plus MIG_{21} and MIG_{12} for the migration model) were estimated in FASTSIMCOAL2.

A total of 40 FASTSIMCOAL runs were performed for each pairwise comparison per species per model, with 100,000-250,000 simulations per likelihood estimation based on the stopping criteria of 0.001 and 10-40 ECM (expectation-conditional maximization). Model comparisons of divergence scenarios were performed on the likelihoods of the best point estimate using Akaike Information Criteria (AIC; Akaike, 1974). The power of each estimated parameter was accessed based on parametric bootstrapping for 100 simulated SFS produced with similar conditions to the empirical SFS (e.g., number of individuals, loci and parameters estimated from the maximum composite-likelihood) for each pairwise comparison in each species. All simulated SFS were analyzed in FASTSIMCOAL using the same settings described for the empirical SFSs, and based on their results we calculated confidence intervals for all parameters in each model. Divergence estimates are given in number of generations. Given their similarity in body size and microhabitat, and the limited natural history information available for most non-pest beetles, we assumed the same generation time for both species.

Results

Illumina sequencing generated >100,000,000 reads for each species, with an average of >1,000,000 retained reads per individual (see Supplementary Table 1 and Supplementary Figures 1-2 for detailed sequencing results). After data processing in STACKS, removal of individuals with a relatively high number of missing reads and applying a threshold of 25% missing data, we retained 4422 loci with a single biallelic SNP loci from 98 *A. labralis* and 1327 from 98 *B. scutellaris*. To maximize the number of SNPs for each analysis, we generated separate datasets in Plink for each geographical subset of the data for both species (Supplementary Table 2).

Biogeographic regions and geographic structure

We detected a strong relationship between geography and genomic divergence, as well as shared points of turnover between geographically distinct genomic clusters for both species. For *A. labralis*, STRUCTURE analyses and Evanno's *ΔK* method indicated *K*=4 as the most probable number of genomic clusters, while *K*=2 was the most strongly supported *K* for *B. scutellaris* (Table 1, Figures 2-3). For both species, admixture was most prevalent at regions of turnover between clusters. The Procrustes analyses indicated a significant, strong association between geography and population genetic divergence for both species, although that relationship was stronger for *A. labralis* (*t* = 0.7597) than for *B. scutellaris* (*t* = 0.5393) (Table 2), consistent with the pattern of more geographically constrained clusters identified by *ΔK.*

For *A. labralis*, STRUCTURE identified distinct clusters in northern, eastern, southern and western South Island, with admixture occurring in places where these clusters meet, including across mountain barriers (Figure 2). Of the four discrete regions, the eastern, southern and western clusters were also evident in the Procrustes results (Figure 4a). Notably, populations from northern South Island in STRUCTURE formed distinct eastern and western sets of genetic clusters on Procrustes, suggesting strong within-region divergence. In contrast, all populations from southern South Island grouped tightly together in PCA space, indicating that they are less divergent than expected based on the distance separating localities. When separate Procrustes analyses were performed for each STRUCTURE region, we recovered a similarly significant, strong association between geography and divergence for each cluster (Table 2, Figure 4a). This hierarchical analysis also revealed a remarkable level of genomic divergence in populations around Kaikoura, as reflected by their distinct positions in PCA space, and this pattern was also detected for *B. scutellaris* (Figure 4b).

For *B. scutellaris*, turnover between the two STRUCTURE clusters occurs between Karamea and Nelson in the north and in southern South Island (Figure 3), with the highest admixture in the region between Haast Pass and Central Otago (Supplementary Figure 4). The Procrustes PCA detected three strong regional clusters: the western group, which includes all the west coast plus the southernmost South Island; the eastern cluster, which includes the east coast south of the Kaikoura Ranges plus the Otago highlands; and the northern cluster, which includes Marlborough north of the Kaikouras, the Tasman Bay and Golden Bay regions of Nelson, and the four North Island populations (Figure 3). This configuration also received the second-highest support in the STRUCTURE analyses (K=3, Table 1). Within the northeastern (K=2) STRUCTURE cluster, an additional K=2 minor clusters divided northern South Island and North Island from the east coast (Kaikoura and southward), in line with the Procrustes results (Figure 3, Supplementary Figures 3-4). Within each of the Procrustes clusters, the relationship between geography and population genetic divergence was highly significant (Table 2) and was stronger than for all *B. scutellaris* populations combined (t = 0.6035, t = 0.6975 and t = 0.5726, respectively). Turnover between the western, northern and eastern clusters was broadly congruent between *B. scutellaris* and *A. labralis*.

Within the western *B. scutellaris* group detected by STRUCTURE and Procrustes, we noted that the individual from Flora Saddle (Mount Arthur, Nelson) strongly dominated the axes of variation within the genomic PCA (Figure 4b). While inclusion or exclusion of this individual had relatively little impact on the Procrustes association (0.6035 vs 0.6249, both highly significant) or membership of the major (K=2) STRUCTURE clusters, it strongly affected the number of minor clusters identified by STRUCTURE within the western group.

With Flora Saddle included, *K*=3 sub-clusters were supported, including a distinct northern cluster in the northern region that includes Flora Saddle, one cluster south of the Westland *Nothofagus* gap, and one that is mostly north of the gap but includes Southland and Stewart Island (Supplementary Figure 4). Excluding the Flora Saddle individual, STRUCTURE analyses of the western cluster identified two geographically coherent minor clusters north and south of the *Nothofagus* gap (Figure 3, Supplementary Figures 3 and 5), which we used in all subsequent analyses.

Spatial dynamics within regions

Tests for geographic expansion within genomically-defined regions using allele frequency patterns (Ψ) indicated different spatial dynamics between species, and among regions for both *A. labralis* and *B. scutellaris*. For *A. labralis*, expansion was detected for the southern and western clusters, but not the north or the east, although a signal of expansion was marginally non-significant for the north (p=0.08). For *B. scutellaris*, recent expansion was detected for the northern, eastern and western clusters; however, when considered separately, the western populations north of the *Nothofagus* gap had a signal of expansion while those to the south did not (Table 3). Kaikoura and Nelson/Karamea (Tasman coast) were inferred as points of origin for the eastern and western clusters, respectively, for both species, although this pattern was not accompanied by a signal of recent expansion for *A. labralis* in both regions (Figures 2d and 3e, Supplementary Figures 6-7). For *B. scutellaris*, we included the North Island individuals as a single population, and results indicate a North Island origin for the northern cluster. For both species, the origin of the southernmost populations was inferred in the Haast region: for *A. labralis*, the origin was at the coast, south of the Haast River mouth, while for *B. scutellaris*, the origin was closer to Haast Pass, although there was no signal of expansion.

Temporal divergence among regions

The model of divergence with migration was more probable than the strict divergence model in all in comparisons (Supplementary Table 3), indicating that dispersal barriers are permeable over time. Beyond this commonality, we failed to detect concordant divergence times across the Southern Alps or across other geographic barriers. Under the conservative assumption of similar numbers of generations per year (see below), divergence across the Southern Alps occurred deeper in the past for *B. scutellaris* than *A. labralis* (5 times older for the full comparison; 2 times older when considering breaks between specific regions) (Figures 2c-d & 3d-e, Table 4; see Supplementary Table 4 for results using the strict divergence model). For *A. labralis*, the deepest divergence among regions occurred between the south and east at ~156,000 generations, with

other divergences ranging from 37,000 to 133,000 generations ago. For *B. scutellaris*, the deepest divergence among STRUCTURE regions separated the east and southwest (~252,000 generations), although the north-west and northeast-northwest divergences were of a similar magnitude (Figure 3e). While there were no distinct patterns in the order of divergence among regions between *A. labralis* and *B. scutellaris*, the oldest breaks for both species appear to delineate east from west: for *A. labralis* the oldest breaks separated the eastern region from its neighbors, while the oldest for *B. scutellaris* separated the two major STRUCTURE CLUSTERS (northeast and southwest). The shallow divergence of ~9,000 generations between *B. scutellaris* populations spanning the *Nothofagus* gap falls outside the 95% bootstrap confidence interval for divergence time, as do estimates for N_{ANC} and N_2. This indicates a lack of power to infer these parameters with confidence, potentially caused by a model misspecification, which suggests an absence of actual divergence across this break (Table 4). Generally low migration rates of less than one individual per generation were estimated for both species, with *B. scutellaris* showing slightly lower rates than *A. labralis*.

The closest available generation time information for these taxa are from laboratory observations for *Scaphisoma castaneum* (Staphylinidae: Scaphidiinae) for which complete developmental time averaged 22 days (Hanley, 1996). Translating this into generation time under natural conditions is difficult because reproductive and developmental rates are likely contingent on environmental conditions and seasonality. Therefore, we avoid explicitly translating our divergence times into calendar years. However, we note that under a conservative estimate of 6 generations per year, which assumes cessation of reproduction over the winter months, the deeper divergences for *B. scutellaris* (Figure 3e) occur around 41,000 years ago while the oldest for *A. labralis* (Figure 2d) are around 22,000-26,000 years ago. With greater numbers of generations (e.g., 12 generations per year) most divergences for *B. scutellaris* would still predate the Holocene period (beginning ~12,000 years ago), whereas even with as few as 3 generations per year, divergences for both species would predate or coincide with the Last Glacial Period. Note that the generations times would have be very dissimilar between these ecologically similar taxa to produce a false pattern of temporal concordance (and there is no evidence to suggest such differences between the species).

Discussion

The dynamic geological histories of regions like New Zealand set the stage for diverse phylogeographic histories among intraspecific populations of widely distributed species, leading to complex patterns of phylogeographic concordance among species which co-occur across large parts of their geographic distributions. We tested

whether SNPs for two widely distributed beetle species showed the impact of similar processes at the scale of South Island (similar orientation and timing of phylogeographic breaks) and within the regions delimited by these barriers (similar spatial dynamics of isolation-by-distance or geographic expansion). While differences between species were apparent at both scales, we found two exciting results: 1) shared phylogeographic breaks between regions were not indicative of shared spatial patterns within regions, suggesting that concordance of patterns within and between species varies between regions and scales of comparison, depending on regional impacts of geography and climate; and 2) congruence in spatial dynamics occurred only in the case of geographic expansion, in regions with a refugium immediately next to an area heavily impacted by glaciation. If these patterns are broadly replicated across the community, they suggest that detection of shared spatial dynamics within regions may be contingent upon that region's history of stability, providing an explicitly process-based framework for when phylogeographic concordance should be expected. Further, our findings reflect the limits of measures of concordance based on divergence *between* lineages or regions in characterizing the extent to which species share responses to historical events. We propose that the spatial dynamics that occur *within* distinct regional lineages offer an additional avenue for identifying the processes leading to phylogeographic concordance. This expanded focus provides historical context for the interpretation of species-level divergence patterns that are otherwise geographically and temporally idiosyncratic.

Phylogeographic breaks: variation in geographic and temporal concordance

In northern and central South Island, both species share the hard barriers of the central Southern Alps, Paparoa and Kaikoura Ranges, delimiting distinct eastern, western and northern genomic clusters. However, different divergence date estimates across these ranges suggest that *A. labralis* and *B. scutellaris* reached these barriers at different times, rather than as a shared divergence event. Given scant knowledge on the life histories of both species, our divergence estimates are left as generations rather than converted to years, preventing an explicit test of the importance of specific geological and climatic events. We also assume that both species undergo a similar number of generations per year, given that adults were collected from similar microhabitats on the same collecting trips. However, even if these species do vary in voltinism, we would still expect the geographic sequence of divergences to be held in common if divergence occurred in synchrony. Although a lack of overall geographical order points to species-specific responses to dispersal opportunities despite similar ecological requirements, there is agreement in the relatively old east-west splits for both species. This potential congruence indicates the importance of the Southern Alps as one of the key drivers of

phylogeographic structure in South Island, with the impacts of this dispersal barrier likely heightened by the distinct refugial dynamics in the eastern and western South Island during the lower Pleistocene (Marske et al., 2012).

In contrast, the orientation of phylogeographic breaks varies in southern South Island, where *A. labralis* has a distinct genomic cluster bounded by the Central Otago Highlands but where the eastern and western clusters of *B. scutellaris* meet and spatially interdigitate. In southwestern South Island, long river valleys forge potential connections through the Southern Alps, with Haast Pass as a low, forested route between the west coast and the region south of the Central Otago Highlands. The importance of the Haast corridor as a potential conduit for dispersal is supported by the STRUCTURE results, inferred dispersal patterns, and for *A. labralis*, the deep divergence between the southern and eastern regions, supporting a western origin for southern populations. Thus, similarity in the orientation of phylogeographic lineages and genomic clusters among these ecologically similar species likely has more to do with the dispersal landscape than the orientation of glacial refugia, with greater interspecific variation in phylogeographic regionalization where dispersal filters are less difficult to traverse (i.e., southern South Island), in line with previous mitochondrial results for these (Marske et al., 2012) and other New Zealand species.

Notably, we found limited support for distinct *B. scutellaris* populations on either side of the *Nothofagus* gap, heightening the mystery of the species' apparent absence from this region of the west coast. Curiously, the evidence for this lack of divergence in western South Island is tied to the genetically distinct Flora Saddle individual (hereafter FS) from northern South Island. First, FS is unremarkable in terms of missing data or genomic admixture, so it most likely has a divergent history that is not well represented in our data, which would explain its effect on the hierarchical STRUCTURE results (Figure 3 vs Supplementary Figure 4b). Mount Arthur, where FS was collected, also yielded the sole specimen of a deeply divergent lineage of another forest litter beetle species (Marske, Leschen, & Buckley, 2011), supporting the idea that there is undetected genetic diversity in this region. Second, only by excluding FS from the hierarchical STRUCTURE analysis do we detect support for the *Nothofagus* gap as a dispersal barrier (Figure 3). Divergence among the resulting clusters is the shallowest across our study, but the estimated divergence time falls outside the 95% confidence interval for this estimate (Table 4), suggesting a lack of support for this western split, in agreement with the Procrustes results and second-best *K* from the STRUCTURE analysis (Table 1). Taken together, our data suggest recent gene flow across or around the *Nothofagus* gap, raising new questions about species dispersal across this glacially impacted area.

Regional dynamics: congruence of expansion events

The intraspecific differences in regional dynamics observed between species indicate that congruent phylogeographic breaks do not indicate congruent processes in the regions they delimit, and each genomically-defined region represents a discrete opportunity for inter- and intra-specific comparisons of regional histories (within and across regions, respectively). Interestingly, the one region that is well-defined for both species by phylogeographic breaks and in which regional spatial dynamics are shared—the west—shows that geographic expansion originates in the area with the best evidence for a large glacial refugium (Karamea) (Alloway et al., 2007; Marske et al., 2012) and expands through an area heavily impacted by glaciation (central west coast) (Figures 2d and 3e). This region's gradient of historical environmental stability, combined with a long, narrow geography, may have shaped a concordance of genomic patterns that are driven by recent dispersal events. In northern and eastern South Island, the other two regions whose boundaries are largely shared between species, we see different regional histories between *A. labralis* and *B. scutellaris*, due to differences in refugial histories and immigration from North Island for *B. scutellaris,* suggesting that absence of a common response to environmental gradients allowed species-specific patterns to emerge. Together, these patterns indicate a process, climate change, and a mechanism, dispersal, likely to impact the detection of phylogeographic concordance in regional spatial dynamics.

In southern South Island, evidence for expansion of both species via the Haast corridor into the region south of the Otago Highlands suggests that climatic instability and dispersal has shaped the southern distributions of both species, despite the lack of shared phylogeographic breaks delimiting this region. For lowland species, southern South Island has been less well studied phylogeographically than the north, likely due to the near absence of glacial refugia, inaccessibility of its southwest corner, and extensive deforestation. However, the Haast corridor has proven important as a potential glacial refugium (Weir, Haddrath, Robertson, Colbourne, & Baker, 2016) and contact zone (Davis, Brav-Cubitt, Buckley, & Leschen, 2019) for lineages of multiple species. For *B. scutellaris*, expansion into the south from the east as well as via Haast highlights that the Otago highlands may be more permeable to some species than the topographic barriers delimiting northern South Island. If additional species share this combination of concordance of process despite variation in colonization pathways, these spatial dynamics provide critical information on the role of immigration in shaping species richness and coexistence patterns in regions heavily impacted by climate change.

Our legacy sampling design (few individuals from each of ~100 localities) does limit our ability to test these complex spatial hypotheses: For the Ψ analyses, localities were aggregated into populations, which

restricts our ability to use a more spatially explicit dispersal landscape, while for the Procrustes analysis, numerous diffuse population clusters that conform strongly or loosely to a pattern of IBD make it difficult to identify where areas with divergent histories may be unduly influencing the pattern (Knowles et al., 2016). An explicit population genetic focus in sampling design will easily alleviate these issues for future studies, allowing a deeper investigation of differences in genomic diversity among localities within regions. However, for the regional scale patterns we present here, our methods already provide a powerful test for differences in the geography of diversification and the circumstances likely to lead to phylogeographic concordance. These analyses leverage the power of reduced-representation library preparation methods for quick, inexpensive data generation which characterizes population-level variation for species lacking other genomic resources (i.e., most insects; Li et al., 2019), as innovations in sequencing and library preparation methods (e.g., Bayona-Vásquez et al., 2019) continue to reduce the cost.

Anticipating phylogeographic concordance: contingent upon climate history?

Our results indicate that lack of range-wide phylogeographic concordance, as measured by the geographic turnover or timing of divergence between lineages, does not rule out the possibility of shared spatial histories within individual regions. Further, variation in the occurrence of different types of concordance may provide insights into the different processes that shape species' histories. We found that the likelihood of detecting phylogeographic concordance is heavily context-dependent and may be based on the strength of the barrier or ecological gradient through their impact on dispersal limitation or facilitation. While dispersal is often invoked as a driver of species-specific rather than concordant phylogeographic patterns (e.g., Marske et al. 2012; Thomaz and Knowles, 2020), our results highlight the role of dispersal opportunities, such as expansion, in driving patterns of similarity in regional spatial dynamics among species.

These explicitly process-based histories, and the expansion of tests for spatial concordance to include patterns that are not related to vicariance, could provide invaluable insights into the history of diversification and community assembly in geologically and climatically dynamic regions. For *A. labralis* and *B. scutellaris*, the combination of species-specific divergences across long term barriers, plus longer relative environmental stability in the north (Marske et al., 2012), suggest that this region has had more time to accumulate forest species, and predicts that the species in this region will have a variety of regional histories—including long-term residents showing isolation-by-distance or local adaptation and recent colonizers showing geographic expansion. In contrast, communities that experienced stronger environmental variation, such as southern South Island, should be skewed toward recent dispersers, yielding a higher likelihood of shared historical

dynamics among species in this region. While this idea remains to be tested at the community level, it suggests a novel expansion of the hypothesis of environmental stability as an engine driving the accumulation of inter- (Mittelbach et al., 2007) and intraspecific diversity (Carnaval et al., 2014; Hewitt, 2000). As well as collecting species and genotypes, long-stable regions may capture a larger diversity of spatial histories, as species may arise locally, persist in these regions over long periods or arrive via dispersal. In contrast, regions which have only recently gained suitable habitats should have younger communities dominated by recent dispersers, potentially arriving via different routes. If replicated across ecologically similar species, these patterns provide a mechanistic interpretation for complex patterns of phylogeographic concordance in geographically and topographically dynamic systems.

Acknowledgements

We gratefully acknowledge Thomas Buckley and Richard Leschen for assistance with obtaining the DNA, Mariah Kenney, Renata Pirani and Raquel Marchan-Rivadeneira for laboratory support, Qixin He, Melisa Olave, Luciana Resende-Moreira, Joyce Prado, Alana Alexander, Greg Newman and Marcos da Cruz for analytical support, and Hayley Lanier, Mike Kaspari, Rosemary Gillespie and three anonymous reviewers for providing invaluable perspectives on key results. This research was supported with funding from the Insect Division in the Museum of Zoology, University of Michigan, Ann Arbor. KAM also thanks the College of Arts and Sciences, University of Oklahoma, and ATT thanks the BRITE postdoctoral fellowship from the Biodiversity Research Centre at the University of British Columbia. Specimens were originally collected under the Landcare Research Global Concession issued by the Department of Conservation (permit number CA-5160-OTH).

Supporting Information

Supplementary methods and results, including four Tables and seven Figures, are included as a single file.

Data Accessibility

RADseq data are archived at the NCBI Sequence Read Archive (BioProject ID: PRJNA655212). Locality data, BioSample accession numbers, and input files and custom scripts for all post-STACKS analyses are available in the Dryad digital repository (https://doi.org/10.5061/dryad.3tx95x6df) and on GitHub (https://github.com/KAMarske/MarskeThomazKnowles_2020).

Author Contributions

KAM and LLK conceived the study, KAM collected the data with input from ATT, KAM and ATT analyzed the data, and all authors contributed to the writing of the manuscript.

Literature Cited

Akaike, H. (1974). A new look at the statistical model identification. *IEEE Transactions on Automatic Control*, *19*(6), 716–723. doi: 10.1109/TAC.1974.1100705

Alloway, B. V., Lowe, D. J., Barrell, D. J. A., Newnham, R. M., Almond, P. C., Augustinus, P. C., … Williams, P. W. (2007). Towards a climate event stratigraphy for New Zealand over the past 30 000 years (NZ-INTIMATE project). *Journal of Quaternary Science*, *22*(1), 9–35.

Avise, J. C., Arnold, J., Ball, R. M., Bermingham, E., Lamb, T., Neigel, J. E., … Saunders, N. C. (1987). Intraspecific Phylogeography: The Mitochondrial DNA Bridge Between Population Genetics and Systematics. *Annual Review of Ecology and Systematics*, *18*(1), 489–522. doi: 10.1146/annurev.es.18.110187.002421

Bayona-Vásquez, N. J., Glenn, T. C., Kieran, T. J., Pierson, T. W., Hoffberg, S. L., Scott, P. A., … Faircloth, B. C. (2019). Adapterama III: Quadruple-indexed, double/triple-enzyme RADseq libraries (2RAD/3RAD). *PeerJ*, *7*, e7724. doi: 10.7717/peerj.7724

Bemmels, J. B., Knowles, L. L., & Dick, C. W. (2019). Genomic evidence of survival near ice sheet margins for some, but not all, North American trees. *Proceedings of the National Academy of Sciences*, 201901656. doi: 10.1073/pnas.1901656116

Bermingham, E., & Moritz, C. (1998). Comparative phylogeography: concepts and applications. *Molecular Ecology*, 367–369.

Binks, R. M., Gibson, N., Ottewell, K. M., Macdonald, B., & Byrne, M. (2019). Predicting contemporary range-wide genomic variation using climatic, phylogeographic and morphological knowledge in an ancient, unglaciated landscape. *Journal of Biogeography*, *46*(3), 503–514. doi: 10.1111/jbi.13522

Boyer, S. L., Baker, J. M., & Giribet, G. (2007). Deep genetic divergences in *Aoraki denticulata* (Arachnida, Opiliones, Cyphophthalmi): A widespread “mite harvestman” defies DNA taxonomy. *Molecular Ecology*, *16*(23), 4999–5016. doi: 10.1111/j.1365-294X.2007.03555.x

Buckley, T. R., Krosch, M., & Leschen, R. A. B. (2015, February 1). Evolution of New Zealand insects: summary and prospectus for future research. *Austral Entomology*, 54(1), 1-27. doi:10.1111/aen.12116

Bunnefeld, L., Hearn, J., Stone, G. N., & Lohse, K. (2018). Whole-genome data reveal the complex history of a diverse ecological community. *Proceedings of the National Academy of Sciences*, *115*(28), E6507–E6515. doi: 10.1073/pnas.1800334115

552 Burbrink, F. T., Chan, Y. L., Myers, E. A., Ruane, S., Smith, B. T., & Hickerson, M. J. (2016). Asynchronous
553 demographic responses to Pleistocene climate change in Eastern Nearctic vertebrates. *Ecology Letters*,
554 *19*(12), 1457–1467. doi: 10.1111/ele.12695
555 Carnaval, A. C., Waltari, E., Rodrigues, M. T., Rosauer, D., VanDerWal, J., Damasceno, R., … Moritz, C. (2014).
556 Prediction of phylogeographic endemism in an environmentally complex biome. *Proceedings of the*
557 *Royal Society B: Biological Sciences*, *281*(1792). doi: 10.1098/rspb.2014.1461
558 Carstens, B. C., & Richards, C. L. (2007). Integrating coalescent and ecological niche modeling in comparative
559 phylogeography. *Evolution*, *61*(6), 1439–1454. doi: 10.1111/j.1558-5646.2007.00117.x
560 Catchen, J., Hohenlohe, P. A., Bassham, S., Amores, A., & Cresko, W. A. (2013). STACKS: an analysis tool set for
561 population genomics. *Molecular Ecology*, *22*(11), 3124–3140. doi: 10.1111/mec.12354
562 Craw, D., Upton, P., Burridge, C. P., Wallis, G. P., & Waters, J. M. (2016). Rapid biological speciation driven by
563 tectonic evolution in New Zealand. *Nature Geoscience*, *9*(2), 140–144. doi: 10.1038/ngeo2618
564 Davis, S. R., Brav-Cubitt, T., Buckley, T. R., & Leschen, R. A. B. (2019). Systematics of the New Zealand Weevil
565 *Etheophanus Broun* (Curculionidae: Molytinae). *Zootaxa*, *4543*(3), 341–374. doi:
566 10.11646/zootaxa.4543.3.2
567 Dennis, A. B., Dunning, L. T., Sinclair, B. J., & Buckley, T. R. (2015). Parallel molecular routes to cold adaptation
568 in eight genera of New Zealand stick insects. *Scientific Reports*, *5*, 13965. doi: 10.1038/srep13965
569 Dray, S., & Dufour, A.-B. (2007). The ade4 Package: Implementing the Duality Diagram for Ecologists. *Journal of*
570 *Statistical Software*, *22*(1), 1–20. doi: 10.18637/jss.v022.i04
571 Earl, D. A., & vonHoldt, B. M. (2012). STRUCTURE HARVESTER: a website and program for visualizing
572 STRUCTURE output and implementing the Evanno method. *Conservation Genetics Resources*, *4*(2),
573 359–361. doi: 10.1007/s12686-011-9548-7
574 Ellis, E. A., Marshall, D. C., Hill, K. B. R., Owen, C. L., Kamp, P. J. J., & Simon, C. (2015). Phylogeography of six
575 codistributed New Zealand cicadas and their relationship to multiple biogeographical boundaries
576 suggest a re-evaluation of the Taupo Line. *Journal of Biogeography*, *42*(9), 1761–1775. doi:
577 10.1111/jbi.12532
578 Espíndola, A., Carstens, B. C., & Alvarez, N. (2014). Comparative phylogeography of mutualists and the effect of
579 the host on the genetic structure of its partners. *Biological Journal of the Linnean Society*, *113*(4),
580 1021–1035. doi: 10.1111/bij.12393

Evanno, G., Regnaut, S., & Goudet, J. (2005). Detecting the number of clusters of individuals using the software STRUCTURE: a simulation study. *Molecular Ecology*, *14*(8), 2611–2620. doi: 10.1111/j.1365-294X.2005.02553.x

Excoffier, L., Dupanloup, I., Huerta-Sánchez, E., Sousa, V. C., & Foll, M. (2013). Robust demographic inference from genomic and SNP data. *PLoS Genetics*, *9*(10), e1003905. doi: 10.1371/journal.pgen.1003905

Excoffier, L., & Foll, M. (2011). fastsimcoal: a continuous-time coalescent simulator of genomic diversity under arbitrarily complex evolutionary scenarios. *Bioinformatics (Oxford, England)*, *27*(9), 1332–1334. doi: 10.1093/bioinformatics/btr124

Fernández, R., & Giribet, G. (2014). Phylogeography and species delimitation in the New Zealand endemic, genetically hypervariable harvestman species, *Aoraki denticulata* (Arachnida, Opiliones, Cyphophthalmi). *Invertebrate Systematics*, *28*(4), 401–414. doi: 10.1071/IS14009

Garrick, R. C., Rowell, D. M., Simmons, C. S., Hillis, D. M., & Sunnucks, P. (2008). Fine-scale phylogeographic congruence despite demographic incongruence in two low-mobility saproxylic springtails. *Evolution*, *62*(5), 1103–1118. doi: 10.1111/j.1558-5646.2008.00349.x

Hanley, R. S. (1996). Immature stages of *Scaphisoma castaneum* Motschulsky (Coleoptera: Staphylinidae: Scaphidiinae), with observations on natural history, fungal hosts and development. *Proceedings of the Entomological Society of Washington*, *98*(1), 36–43.

Hanrahan, S. J., & Johnston, J. S. (2011). New genome size estimates of 134 species of arthropods. *Chromosome Research*, *19*(6), 809. doi: 10.1007/s10577-011-9231-6

He, Q., & Knowles, L. L. (2016). Identifying targets of selection in mosaic genomes with machine learning: applications in *Anopheles gambiae* for detecting sites within locally adapted chromosomal inversions. *Molecular Ecology*, *25*(10), 2226–2243. doi: 10.1111/mec.13619

He, Q., Prado, J. R., & Knowles, L. L. (2017). Inferring the geographic origin of a range expansion: Latitudinal and longitudinal coordinates inferred from genomic data in an ABC framework with the program X - ORIGIN. *Molecular Ecology*, *26*(24), 6908–6920. doi: 10.1111/mec.14380

Hewitt, G. (2000). The genetic legacy of the Quaternary ice ages. *Nature*, *405*(6789), 907–913. doi: 10.1038/35016000

Jombart, T. (2008). adegenet: a R package for the multivariate analysis of genetic markers. *Bioinformatics*, *24*(11), 1403–1405. doi: 10.1093/bioinformatics/btn129

Knowles, L. L., Massatti, R., He, Q., Olson, L. E., & Lanier, H. C. (2016). Quantifying the similarity between genes and geography across Alaska's alpine small mammals. *Journal of Biogeography*, *43*(7), 1464–1476. doi: 10.1111/jbi.12728

Kopelman, N. M., Mayzel, J., Jakobsson, M., Rosenberg, N. A., & Mayrose, I. (2015). Clumpak: a program for identifying clustering modes and packaging population structure inferences across K. *Molecular Ecology Resources*, *15*(5), 1179–1191. doi: 10.1111/1755-0998.12387

Leschen, R. A. B., Buckley, T. R., Harman, H. M., & Shulmeister, J. (2008). Determining the origin and age of the Westland beech (*Nothofagus*) gap, New Zealand, using fungus beetle genetics. *Molecular Ecology*, *17*(5), 1256–1276. doi: 10.1111/j.1365-294X.2007.03630.x

Li, F., Zhao, X., Li, M., He, K., Huang, C., Zhou, Y., … Walters, J. R. (2019). Insect genomes: progress and challenges. *Insect Molecular Biology*, *28*(6), 739–758. doi: 10.1111/imb.12599

Lynch, M. (2010). Evolution of the mutation rate. *Trends in Genetics : TIG*, *26*(8), 345–352. doi: 10.1016/j.tig.2010.05.003

Manuel, M. de, Kuhlwilm, M., Frandsen, P., Sousa, V. C., Desai, T., Prado-Martinez, J., … Marques-Bonet, T. (2016). Chimpanzee genomic diversity reveals ancient admixture with bonobos. *Science*, *354*(6311), 477–481. doi: 10.1126/science.aag2602

Marshall, D. C., Hill, K. B. R., Fontaine, K. M., Buckley, T. R., & Simon, C. (2009). Glacial refugia in a maritime temperate climate: Cicada (*Kikihia subalpina*) mtDNA phylogeography in New Zealand. *Molecular Ecology*, *18*(9), 1995–2009. doi: 10.1111/j.1365-294X.2009.04155.x

Marshall, D. C., Hill, K. B. R., Marske, K. A., Chambers, C., Buckley, T. R., & Simon, C. (2012). Limited, episodic diversification and contrasting phylogeography in a New Zealand cicada radiation. *BMC Evolutionary Biology*, *12*(1), 177. doi: 10.1186/1471-2148-12-177

Marske, K. A., Leschen, R. A. B., Barker, G. M., & Buckley, T. R. (2009). Phylogeography and ecological niche modelling implicate coastal refugia and trans-alpine dispersal of a New Zealand fungus beetle. *Molecular Ecology*, *18*(24), 5126–5142. doi: 10.1111/j.1365-294X.2009.04418.x

Marske, K. A., Leschen, R. A. B., & Buckley, T. R. (2011). Reconciling phylogeography and ecological niche models for New Zealand beetles: Looking beyond glacial refugia. *Molecular Phylogenetics and Evolution*, *59*(1), 89–102. doi: 10.1016/j.ympev.2011.01.005

Marske, K. A., Leschen, R. A. B., & Buckley, T. R. (2012). Concerted versus independent evolution and the search for multiple refugia: Comparative phylogeography of four forest beetles. *Evolution*, *66*(6), 1862–1877. doi: 10.1111/j.1558-5646.2011.01538.x

641 Marske, K. A., Rahbek, C., & Nogués-Bravo, D. (2013). Phylogeography: Spanning the ecology-evolution
642 continuum. *Ecography*, *36*(11), 1169–1181. doi: 10.1111/j.1600-0587.2013.00244.x
643 Massatti, R., & Knowles, L. L. (2016). Contrasting support for alternative models of genomic variation based on
644 microhabitat preference: species-specific effects of climate change in alpine sedges. *Molecular Ecology*,
645 *25*(16), 3974–3986. doi: 10.1111/mec.13735
646 McCulloch, G. A., Wallis, G. P., & Waters, J. M. (2010). Onset of glaciation drove simultaneous vicariant isolation
647 of alpine insects in New Zealand. *Evolution*, *64*(7), 2033–2044. doi: 10.1111/j.1558-5646.2010.00980.x
648 Mittelbach, G. G., Schemske, D. W., Cornell, H. V., Allen, A. P., Brown, J. M., Bush, M. B., … Turelli, M. (2007).
649 Evolution and the latitudinal diversity gradient: Speciation, extinction and biogeography. *Ecology*
650 *Letters*, *10*(4), 315–331. doi: 10.1111/j.1461-0248.2007.01020.x
651 Moritz, C., Hoskin, C. J., MacKenzie, J. B., Phillips, B. L., Tonione, M., Silva, N., … Graham, C. H. (2009).
652 Identification and dynamics of a cryptic suture zone in tropical rainforest. *Proceedings. Biological*
653 *Sciences / The Royal Society*, *276*(1660), 1235–1244. doi: 10.1098/rspb.2008.1622
654 Oksanen, J., Blanchet, F. Guillaume, Friendly, M., Kindt, R., Legendre, P., McGlinn, D., … Wagner, H. (2018).
655 vegan: Community Ecology Package. (Version R package version 2.5-1.). Retrieved from
656 https://CRAN.R-project.org/package=vegan
657 O'Neill, S. B., Buckley, T. R., Jewell, T. R., & Ritchie, P. A. (2009). Phylogeographic history of the New Zealand
658 stick insect *Niveaphasma annulata* (Phasmatodea) estimated from mitochondrial and nuclear loci.
659 *Molecular Phylogenetics and Evolution*, *53*(2), 523–536. doi: 10.1016/j.ympev.2009.07.007
660 Oswald, J. A., Overcast, I., Mauck, W. M., Andersen, M. J., & Smith, B. T. (2017). Isolation with asymmetric gene
661 flow during the nonsynchronous divergence of dry forest birds. *Molecular Ecology*, *26*(5), 1386–1400.
662 doi: 10.1111/mec.14013
663 Papadopoulou, A., & Knowles, L. L. (2015). Genomic tests of the species-pump hypothesis: Recent island
664 connectivity cycles drive population divergence but not speciation in Caribbean crickets across the
665 Virgin Islands. *Evolution; International Journal of Organic Evolution*, *69*(6), 1501–1517. doi:
666 10.1111/evo.12667
667 Papadopoulou, A., & Knowles, L. L. (2016). Toward a paradigm shift in comparative phylogeography driven by
668 trait-based hypotheses. *Proceedings of the National Academy of Sciences*, *113*(29), 8018. doi:
669 10.1073/pnas.1601069113

Paz, A., Spanos, Z., Brown, J. L., Lyra, M., Haddad, C., Rodrigues, M., & Carnaval, A. (2018). Phylogeography of Atlantic Forest glassfrogs (*Vitreorana*): when geography, climate dynamics and rivers matter. *Heredity*, 1. doi: 10.1038/s41437-018-0155-1

Peres-Neto, P. R., & Jackson, D. A. (2001). How well do multivariate data sets match? The advantages of a Procrustean superimposition approach over the Mantel test. *Oecologia*, *129*(2), 169–178. doi: 10.1007/s004420100720

Peter, B. M., & Slatkin, M. (2013). Detecting range expansions from genetic data. *Evolution*, *67*(11), 3274–3289. doi: 10.1111/evo.12202

Peter, B. M., & Slatkin, M. (2015). The effective founder effect in a spatially expanding population. *Evolution*, *69*(3), 721–734. doi: 10.1111/evo.12609

Peterson, B. K., Weber, J. N., Kay, E. H., Fisher, H. S., & Hoekstra, H. E. (2012). Double Digest RADseq: An Inexpensive Method for De Novo SNP Discovery and Genotyping in Model and Non-Model Species. *PLOS ONE*, *7*(5), e37135. doi: 10.1371/journal.pone.0037135

Pierce, A. A., Zalucki, M. P., Bangura, M., Udawatta, M., Kronforst, M. R., Altizer, S., … de Roode, J. C. (2014). Serial founder effects and genetic differentiation during worldwide range expansion of monarch butterflies. *Proceedings. Biological Sciences*, *281*(1797). doi: 10.1098/rspb.2014.2230

Pons, J., Fujisawa, T., Claridge, E. M., Anthony Savill, R., Barraclough, T. G., & Vogler, A. P. (2011). Deep mtDNA subdivision within Linnean species in an endemic radiation of tiger beetles from New Zealand (genus *Neocicindela*). *Molecular Phylogenetics and Evolution*, *59*(2), 251–262. doi: 10.1016/j.ympev.2011.02.013

Prates, I., Xue, A. T., Brown, J. L., Alvarado-Serrano, D. F., Rodrigues, M. T., Hickerson, M. J., & Carnaval, A. C. (2016). Inferring responses to climate dynamics from historical demography in neotropical forest lizards. *Proceedings of the National Academy of Sciences*, *113*(29), 7978. doi: 10.1073/pnas.1601063113

Pritchard, J. K., Stephens, M., & Donnelly, P. (2000). Inference of Population Structure Using Multilocus Genotype Data. *Genetics*, *155*(2), 945.

Purcell, S., Neale, B., Todd-Brown, K., Thomas, L., Ferreira, M. A. R., Bender, D., … Sham, P. C. (2007). PLINK: A Tool Set for Whole-Genome Association and Population-Based Linkage Analyses. *American Journal of Human Genetics*, *81*(3), 559–575.

Pyron, R. A., & Burbrink, F. T. (2010). Hard and soft allopatry: Physically and ecologically mediated modes of geographic speciation. *Journal of Biogeography*, *37*(10), 2005–2015. doi: 10.1111/j.1365-2699.2010.02336.x

Rissler, L. J. (2016). Union of phylogeography and landscape genetics. *Proceedings of the National Academy of Sciences*, *113*(29), 8079–8086. doi: 10.1073/pnas.1601073113

Rissler, L. J., & Smith, W. H. (2010). Mapping amphibian contact zones and phylogeographical break hotspots across the United States. *Molecular Ecology*, *19*(24), 5404–5416. doi: 10.1111/j.1365-294X.2010.04879.x

Salces-Castellano, A., Patiño, J., Alvarez, N., Andújar, C., Arribas, P., Braojos-Ruiz, J. J., … Emerson, B. C. (2019). Climate drives community-wide divergence within species over a limited spatial scale: evidence from an oceanic island. *Ecology Letters*. doi: 10.1111/ele.13433

Satler, J. D., & Carstens, B. C. (2019). The *Sarracenia alata* pitcher plant system and obligate arthropod inquilines should be considered an evolutionary community. *Journal of Biogeography*, *46*(2), 485–496.

Smith, B. T., McCormack, J. E., Cuervo, A. M., Hickerson, Michael. J., Aleixo, A., Cadena, C. D., … Brumfield, R. T. (2014). The drivers of tropical speciation. *Nature*, *515*, 406.

Smith, C. I., Tank, S., Godsoe, W., Levenick, J., Strand, E., Esque, T., & Pellmyr, O. (2011). Comparative phylogeography of a coevolved community: Concerted population expansions in Joshua trees and four Yucca moths. *PLoS ONE*, *6*(10). doi: 10.1371/journal.pone.0025628

Thomaz, A T, Malabarba, L. R., & Knowles, L. L. (2017). Genomic signatures of paleodrainages in a freshwater fish along the southeastern coast of Brazil: genetic structure reflects past riverine properties. *Heredity*, *119*(4), 287–294. doi: 10.1038/hdy.2017.46

Thomaz, Andréa T., & Knowles, L. L. (2020). Common barriers, but temporal dissonance: Genomic tests suggest ecological and paleo-landscape sieves structure a coastal riverine fish community. *Molecular Ecology*, *29*(4), 783–796. doi: 10.1111/mec.15357

Tsai, Y.-H. E., & Manos, P. S. (2010). Host density drives the postglacial migration of the tree parasite, *Epifagus virginiana*. *Proceedings of the National Academy of Sciences*, *107*(39), 17035. doi: 10.1073/pnas.1006225107

Wallis, G. P., & Trewick, S. A. (2009). New Zealand phylogeography: Evolution on a small continent. *Molecular Ecology*, *18*(17), 3548–3580. doi: 10.1111/j.1365-294X.2009.04294.x

Wallis, G. P., Waters, J. M., Upton, P., & Craw, D. (2016). Transverse Alpine Speciation Driven by Glaciation. *Trends in Ecology & Evolution*, *31*(12), 916–926. doi: 10.1016/j.tree.2016.08.009

Wang, C., Szpiech, Z. A., Degnan, J. H., Jakobsson, M., Pemberton, T. J., Hardy, J. A., … Rosenberg, N. A. (2010). Comparing spatial maps of human population-genetic variation using Procrustes analysis. *Statistical Applications in Genetics and Molecular Biology*, *9*(1), Article 13. doi: 10.2202/1544-6115.1493

Wang, C., Zöllner, S., Rosenberg, N. A., Weinblatt, M., & Shadick, N. (2012). A Quantitative Comparison of the Similarity between Genes and Geography in Worldwide Human Populations. *PLoS Genetics*, *8*(8), e1002886. doi: 10.1371/journal.pgen.1002886

Weir, J. T., Haddrath, O., Robertson, H. A., Colbourne, R. M., & Baker, A. J. (2016). Explosive ice age diversification of kiwi. *Proceedings of the National Academy of Sciences*, *113*(38), E5580–E5587. doi: 10.1073/pnas.1603795113

Tables

Table 1: Summary of STRUCTURE results for *A. labralis, B. scutellaris*, and the two genomic clusters within *B. scutellaris*. For each analysis, we report the two most likely *K*-values and corresponding *ΔK*. For *B. scutellaris*, the second-best K recovers the three regional clusters identified by the Procrustes analysis, and for southwestern South Island, the second-best K including Flora Saddle recovers the same regional clusters as the first K when Flora Saddle is excluded. South Island and North Island are abbreviated as SI and NI, respectively.

Species and regions	Best *K*	*ΔK*	Second-best *K*	*ΔK*
Agyrtodes labralis	4	367.007	2	16.957
Brachynopus scutellaris	2	5528.913	3	761.399
B. scutellaris, northeast SI & NI	2	3569.913	3	31.821
B. scutellaris, southwest SI				

Including Flora Saddle	3	7138.363	2	396.120
Excluding Flora Saddle	2	700.425	4	16.605

Table 2: Summary of Procrustes results for *A. labralis*, *B. scutellaris*, and three geographical clusters within *B. scutellaris*. We present the strength of association (represented by the *t*-value; see Wang et al. 2010) in a symmetric Procrustes rotation between genomic differentiation and geography, based on 10,000 permutations. All associations are highly significant ($t<0.001$). Geographic and genomic associations with climate are shown in Supplementary Table 3.

Species and regions	Geography
Agyrtodes labralis	0.76 ***
A. labralis, northern SI	0.72***
A. labralis, eastern SI	0.70***
A. labralis, southern SI	0.80***
A. labralis, western SI	0.80***
Brachynopus scutellaris	0.54 ***
B. scutellaris, northern SI	0.70 ***
B. scutellaris, eastern SI	0.57 ***
B. scutellaris, western SI	0.60 ***
B. scutellaris, NW SI *(excl. Flora Saddle)*	0.66***
B. scutellaris, SW SI	0.80***

759

760 **Table 3**: Inferred geographic origins and results of the test for geographic expansion, where *q* is the strength of
761 the directionality index, R100 is the estimated decrease in genomic diversity over 100 km, and rsq and *p* are
762 the correlation coefficient and p-value for the most likely geographic origin, respectively. N pop is the number
763 of populations included in each analysis after aggregating localities; due to this aggregation, we report an area
764 of origin rather than geographic coordinates. For *B. scutellaris*, 'with FS' and 'no FS' indicate inclusion and
765 exclusion of the individual from Flora Saddle.

Species, region	Origin	*q*	R100	rsq	*p*	N pop
A. labralis, north	Marlborough	0.0003	0.9482	0.4695	0.0803	4
A. labralis, east	Kaikoura	0.0000	0.9965	-0.0979	0.6685	5
A. labralis, south	Haast	0.0003	0.9374	0.8383	**0.0000**	7
A. labralis, west	Nelson	0.0001	0.9732	0.6242	**0.0000**	8
B. scutellaris, north	North Island	0.0008	0.8687	0.6567	**0.0314**	4
B. scutellaris, east	Kaikoura	0.0003	0.9451	0.2975	**0.0207**	6
B. scutellaris, west (with FS)	Nelson	0.0002	0.9619	0.5668	**0.0000**	13
B. scutellaris, west (no FS)	Karamea	0.0002	0.9648	0.4769	**0.0000**	12
B. scutellaris, northwest (no FS)	Karamea	0.0012	0.8060	0.6346	**0.0035**	5
B. scutellaris, southwest	Haast Pass	0.0000	0.9956	-0.0454	0.7211	7

766

767 **Table 4 (next page):** FASTSIMCOAL2 results for the Divergence with Migration model per species for
768 each geographic division, including the point estimate and 95% confidence interval in parentheses for
769 each demographic parameter. Included are the number of individuals per population and total
770 number of loci used to calculate each site frequency spectrum (SFS) that were used to infer the
771 population size for one population (N_2), ancestral population size (N_{ANC}), divergence time (T_{DIV}) and
772 migration rate in each direction (*MIG*). Population size N_1 (from the population indicated in bold) was

773 directly estimated from the empirical data based on the reported π for variant and invariant sites and
774 the estimated μ for each species. Point estimates indicated by * fall outside the confidence intervals,
775 indicating uncertainty.

776

Species	Scenario	Inds per Pop	Loci	π	N_1	N_2	N_{ANC}	*MIG*	T_{DIV} (in generations)
A. labralis	Main (East-**West**)	15	3061	0.0028	95238	33667 (24898 - 50175)	11924 (10610 - 735187)	1.13E-05 - 2.99E-06 (3.7E-6 - 2.0E-5; 8.9E-7 - 9.1E-6)	91670 (61454 - 2050616)
	East-South	15	1221	0.0021	71429	41935 (35610 - 59496)	2074* (3752 - 244187)	3.66E-06 - 1.10E-06 (2.7E-6 - 6.2E-6; 3.2E-7 - 1.9E-6)	155577 (76773 - 1762852)
	East-**West**	15	1575	0.0027	91837	39489 (27563 - 47927)	5256 (3304 - 774333)	8.33E-06 - 2.15E-06 (6.0E-6 - 1.5E-5; 7.3E-7 - 2.7E-6)	133387 (72427 - 1876640)
	West-South	15	3114	0.0027	91837	17993 (12185 - 25553)	3571 (2519 - 825158)	5.20E-06 - 1.26E-06 (8.3E-7 - 2.1E-5; 3.2E-9 - 1.7E-5)	36667 (32097 - 1856275)
	North-**East**	15	2486	0.0021	71429	1501984 (1231559 - 1849091)	72660 (54711 - 130503)	3.21E-06 - 6.21E-08 (1.2E-6 - 3.8E-6; 5.0E-11 - 7.0E-6)	110427 (93852 - 1194136)
	North-**West**	15	4317	0.0027	91837	610055 (537652 - 698536)	241010 (182866 - 295873)	9.97E-07 - 2.50E-06 (5.1E-7 - 1.3E-6; 1.7E-6 - 3.6E-6)	65852 (61221 - 75394)
B. scutellaris	Main (East-**West**)	15	1251	0.0024	114286	117511 (100939 - 146716)	15350* (17978 - 686059)	1.80E-07 - 3.76E-06 (3.9E-9 - 3.1E-7; 3.3E-6 - 4.3E-6)	561751 (223080 - 1560904)
	East-South	15	666	0.0011	52381	25470 (18085 - 35428)	39228 (24139 - 842880)	3.74E-06 - 8.24E-06 (2.3E-6 - 4.9E-6; 5.1E-6 - 1.2E-5)	251657 (60466 - 1768380)
	East-**West**	15	848	0.0026	123810	59483 (41426 - 76558)	5207 (2199 - 594384)	2.65E-06 - 7.93E-09 (1.7E-6 - 6.0E-6; 7.2E-10 - 9.3E-8)	240992 (155578 - 2043782)
	West-South	15	4544	0.0026	123810	8410* (8525 - 17034)	1021* (1061 - 841418)	5.54E-05 - 5.70E-06 (1.4E-5 - 5.0E-5; 1.6E-9 - 9.0E-5)	8966* (9187 - 1929744)
	East-North (with NI)	15	1089	0.0011	52381	481711 (394411 - 640717)	35047 (23903 - 643312)	2.75E-06 - 3.75E-07 (2.5E-9 - 4.4E-6; 2.4E-10 - 1.3E-5)	58214 (50473 - 1588498)
	West-North (with NI)	15	1156	0.0026	123810	611636 (487072 - 732192)	303600 (82335 - 547474)	8.85E-08 - 7.79E-07 (1.4E-9 - 2.2E-7; 4.0E-7 - 1.2E-6)	227470 (191877 - 298561)
	East-North (only SI)	15,10	1189	0.0011	52381	298750 (225570 - 345060)	31080 (14270 - 698721)	1.91E-06 - 7.71E-07 (1.4E-7 - 2.6E-6; 3.1E-7 - 1.0E-5)	89286 (72090 - 1432082)
	West-North (only SI)	15,10	1375	0.0026	123810	427834 (376395 - 535374)	165513 (8538 - 381054)	2.74E-07 - 7.95E-07 (6.1E-8 - 5.3E-7; 4.5E-7 - 9.9E-7)	247928 (194585 - 334500)

Figure Captions

Figure 1: Map of South Island geographic features referenced in this study, and major analyses used to quantify phylogeographic breaks between regions and spatial dynamics within regions. Key topographic barriers are highlighted in blue, and glacial refugia previously inferred for these species are indicated in green. The solid green arrow indicates a forest refugium modelled via diverse climate proxies (Alloway et al., 2007), while the dotted arrows indicate additional refugia inferred by Species Distribution Models for these species (Marske et al., 2012).

Figure 2: Geographical population structure, divergence times (in thousands of generations) and summaries of regional histories for *Agyrtodes labralis*. a) Four major STRUCTURE clusters for *A. labralis*, with biogeographic regions ordered in a clockwise direction around the South Island beginning at Kaikoura. b) Geographic distribution of STRUCTURE clusters. c) Divergence times between eastern and western South Island for *A. labralis*. Southland populations were grouped with western South Island due to their separation from the east by the Otago highlands. d) Divergence times among geographically contiguous STRUCTURE clusters for *A. labralis,* and regional histories estimated by the directionality index. The geographic origin of each region is indicated by a circle; circles with arrows indicate the direction of range expansion while circles with black dots indicate regions for which recent expansion was not supported.

Figure 3: Geographical population structure, divergence times (in thousands of generations) and summaries of regional histories for *Brachynopus scutellaris*. a) Two major and b) four minor STRUCTURE clusters for *B. scutellaris*. c) Geographic distribution of STRUCTURE clusters. Flora Saddle is indicated in a) and c) with a red asterisk, and minor clusters shown were estimated with that individual excluded; results with it included are shown in Supplementary Figure 4. All North Island localities (3 not shown) belong to the northern (dark blue) cluster. d) Divergence time between eastern and western South Island, using the same geographical break as for *A. labralis*. e) Divergence times among geographically contiguous minor STRUCTURE clusters and regional histories for *B. scutellaris*. Regional dynamics are shown for

798 eastern, northern and western South Island plus north and south of the *Nothofagus* gap. The blue arrow in northern South Island indicates
799 expansion into the region from North Island.
800
801 **Figure 4:** Results of the Procrustes analysis comparing the spatial orientation between geography and genomic divergence for *Agyrtodes*
802 *labralis* and *Brachynopus scutellaris.* a) Procrustes transformation for all *A. labralis* localities and for the four STRUCTURE clusters, with
803 colors as in Figure 2. Triangles indicate individual sampling localities while circles indicate their relative positions within the genomic PCA.
804 The orientation of the dots and the length of the lines connecting the triangles and dots indicate departure from expectations based on
805 geographic orientation: for example, the southern (yellow) populations are more similar to each other than expected based on the
806 geographic distance between localities, while in the eastern (teal) cluster, the individuals from the Kaikoura region are strongly divergent
807 from each other, despite their geographic proximity. b) Procrustes transformation for all *B. scutellaris* localities and for the three genomic
808 clusters identified (excluding individuals from the NI). Coloration follows Figure 3, although the Procrustes indicated only one western
809 cluster spanning the west coast. Results for separate runs of the two minor western clusters are shown in Supplementary Figure 5.

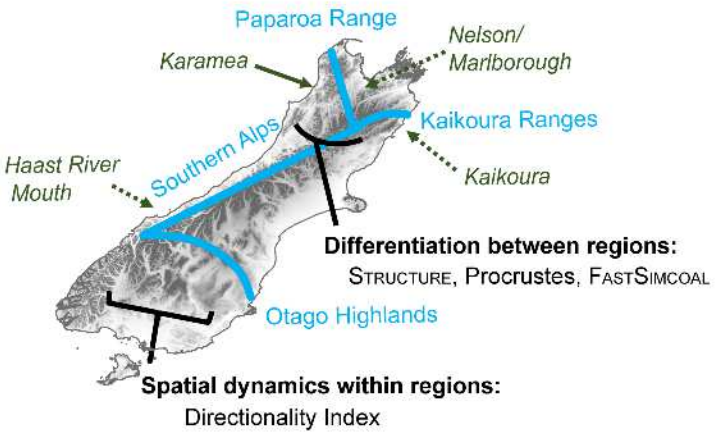

mec_15655_f1.tif

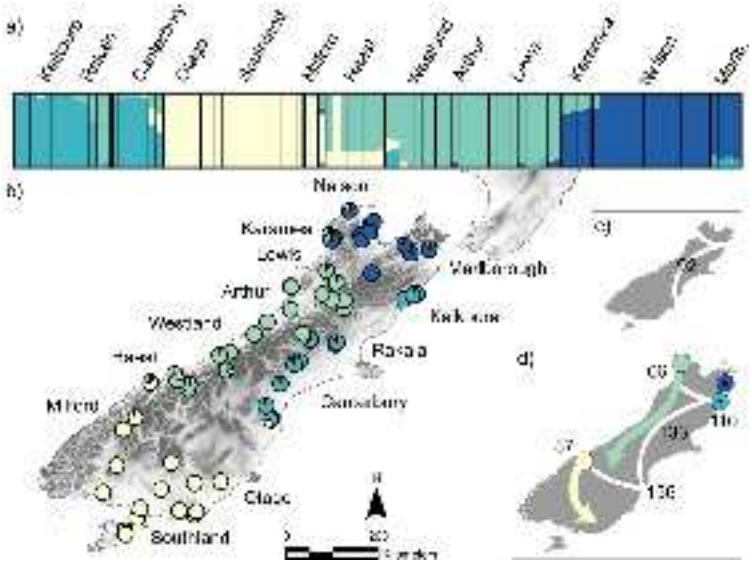

mec_15655_f2.tif

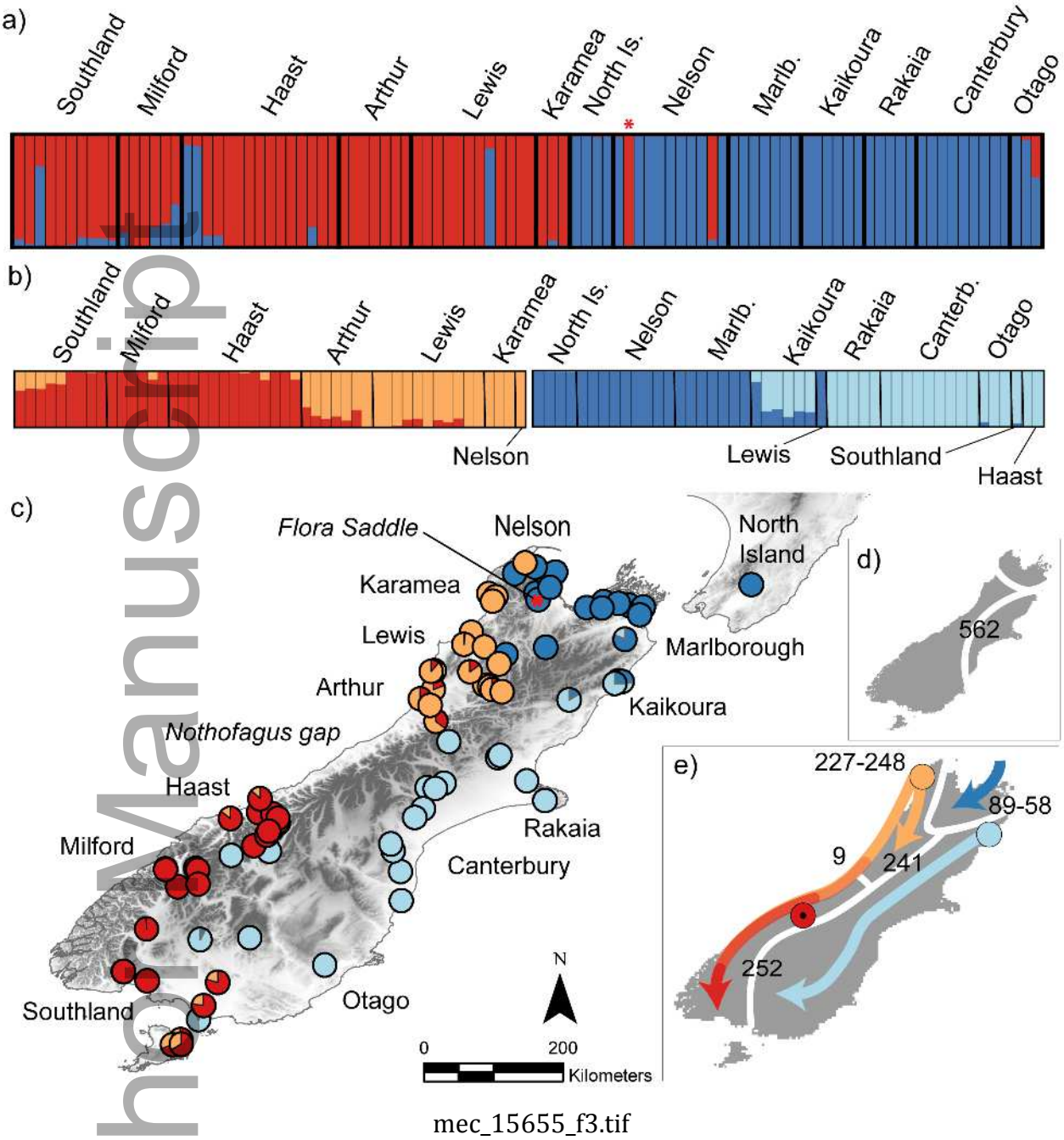

mec_15655_f3.tif

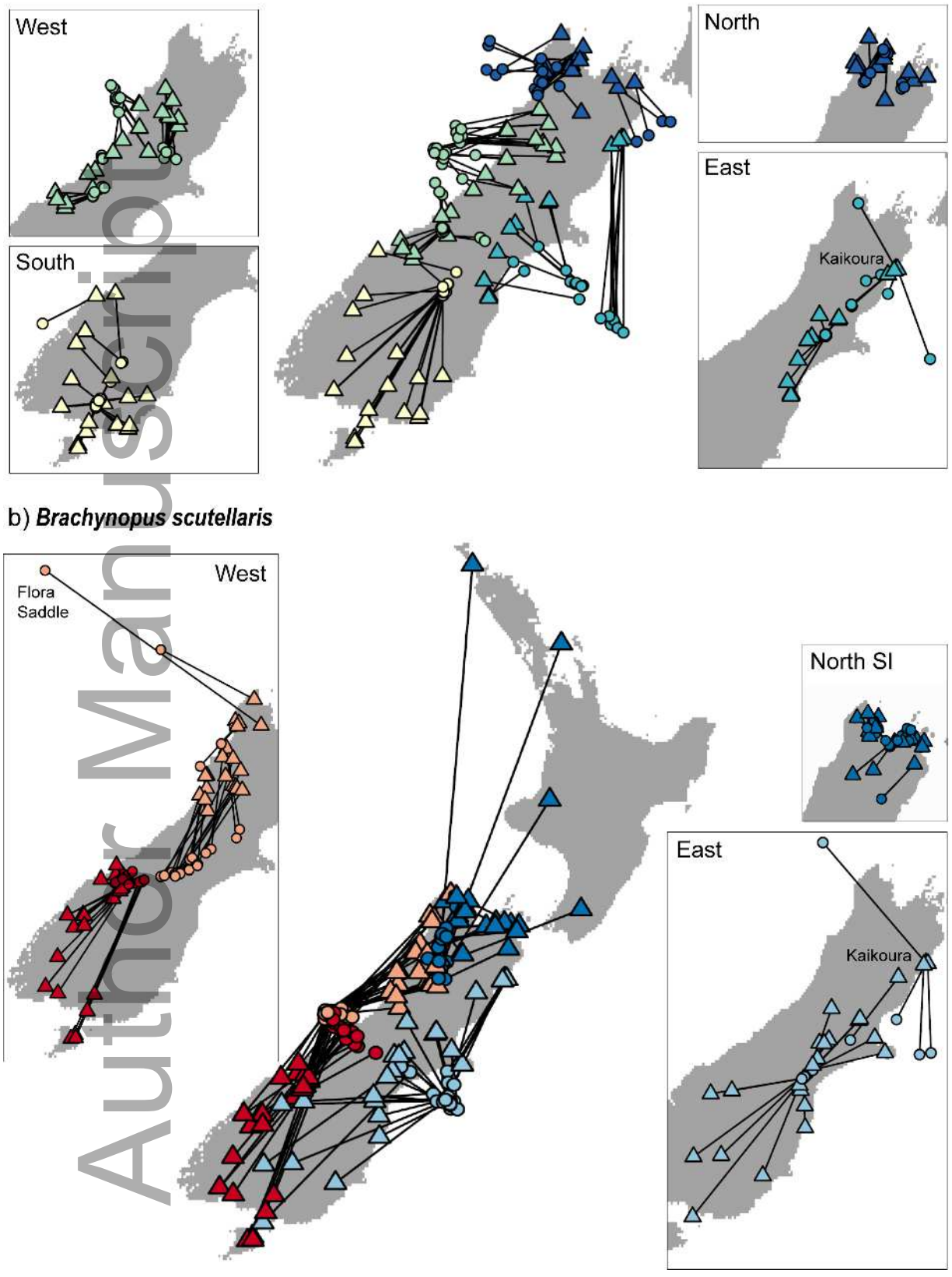

mec_15655_f4.tif